

Enhanced thrust and speed revealed in the forward flight of a butterfly with transient body translation

Yueh-Han John Fei and Jing-Tang Yang*

Department of Mechanical Engineering, National Taiwan University, Taipei 10617, Taiwan

(Received 24 May 2015; published 4 September 2015)

A butterfly with broad wings, flapping at a small frequency, flies an erratic trajectory at an inconstant speed. A large variation of speed within a cycle is observed in the forward flight of a butterfly. A self-propulsion model to simulate a butterfly is thus created to investigate the transient translation of the body; the results, which are in accordance with experimental data, show that the shape of the variation of the flight speed is similar to a sinusoidal wave with a maximum ($J = 0.89$) at the beginning of the downstroke, and a decrease to a minimum ($J = 0.17$) during a transition from downstroke to upstroke; the difference between the extrema of the flight speed is enormous in a flapping cycle. At a high speed, a clapping motion of the butterfly wings decreases the generation of drag. At a small speed, a butterfly is able to capture the induced wakes generated in a downstroke, and effectively generates a thrust at the beginning of an upstroke. The wing motion of a butterfly skillfully interacts with its speed so as to enable an increased speed with the same motion. Considering a butterfly to fly in a constant inflow leads to either an underestimate of its speed or an overestimate of its generated lift, which yields an inaccurate interpretation of the insect's flight. Our results reveal the effect of transient translation on a butterfly in forward flight, which is especially important for an insect with a small flapping frequency.

DOI: [10.1103/PhysRevE.92.033004](https://doi.org/10.1103/PhysRevE.92.033004)

PACS number(s): 47.63.mf, 47.85.Gj, 47.85.lb, 45.40.Aa

I. INTRODUCTION

Insects, the most ancient flyers on planet earth, have evolved during more than 400 million years of natural selection in a harsh environment, and have gradually developed a sophisticated wing structure and kinematics. Repeatedly flapping their wings in the air, an insect generates aerodynamic forces to stay aloft and to perform remarkable flight actions, such as hovering, takeoff, or turning sharply. Understanding the aerodynamics of insect flight may lead to new ways to create or to design a micro air vehicle (MAV).

Differently from an aircraft with fixed wings, an insect generates aerodynamic forces in complicated manners that involve interaction between the fluid and the moving wings. To investigate the difficult associated problems, experimental and computational approaches are the most common ways to reenact in a laboratory the motion of an insect in flight. In an experimental approach, dynamically scaled robotics are placed in a wind or water tunnel to mimic the flying motion of an insect in air [1–3]. In contrast, in computational approaches, a calculation of the wing motion in the fluid allows one to undertake a detailed analysis of the flow field around the insect wings at each moment [4–6]. With these tools, several transient flight mechanisms such as attachment of a leading-edge vortex (LEV) [1,4,7,8], wake capture [3,9], wing rotation [10,11] and a *clap-and-fling* mechanism [12,13] have been proposed to explain the large transient forces generated during an insect's flight. The flight conditions become, however, much simplified during this analysis [7,14–17]: The sample is anchored or fixed in space and the flight speed is replaced with a constant inflow. No matter whether in an experimental or a computational approach, the speed of an insect in flight is seldom rigorously investigated but is treated as a value, which might lead to an inaccurate estimate

and interpretation of the forces generated on a flying insect, particularly a flyer with a small flapping frequency such as a butterfly.

The behavior of a butterfly in flight is unique, and has several distinguishing features among insects. A butterfly flies with a small frequency of flapping and with large wings in a pair; the small flapping frequency leads to a time scale of body response larger than for other insects [18]. The fore and hind wings partly overlap and move simultaneously like one broad wing, which enable the insect to generate large aerodynamic forces abruptly in each stroke. Such a generation and time scale have been regarded as the main cause of the erratic trajectory and large variation of speed [18]. The small flapping frequency of a butterfly also causes a comparable flight speed and wing speed in forward flight; the advance ratio recorded in the forward flight of a butterfly in nature is about 0.9 [19], which indicates that the velocity of the wing is near the flight speed. The aerodynamic forces generated by a butterfly are not only dominated by the flapping motion but also sensitive to the flight speed. Another salient feature of a butterfly is that it invariably presses together its wings at the end of each upstroke. This mechanism, *clap-and-fling*, can not only enhance the lift during flight; the fluid squeezed from that clapping motion can also provide additional thrust for an insect [12,20,21]. Such an aerodynamic benefit is commonly noted for a tiny insect, but, curiously, is rarely adopted by a larger insect [17,20]. The effect of *clap-and-fling* mechanics on the flight of a butterfly has not been clearly explained, and might have a close relation with their transient flight. A butterfly in nature is observed to fly with an unstable motion and an erratic trajectory; the transient translation of the body is necessary but rarely discussed.

The transient flight dynamic of a butterfly has aroused attention; the study of the flight of a butterfly is no longer limited to a discussion of the wing kinematics, but includes also an analysis of the rotational and translational body motion. This flight has been proved to couple with manifold

*jtyang@ntu.edu.tw

aerodynamic mechanisms to improve the performance [22]. Using an artificial butterfly, Tanaka and Shimoyama [6] investigated the stability related to the pitching angle of a butterfly in forward flight. Contriving a light microelectromechanical system (MEMS), Takahashi *et al.* [23] measured directly the differential pressure of the flapping wings; in their results, they found that a periodic differential pressure is generated during the butterfly takeoff, and a large variation of flight speed ($\Delta U = 0.80$ m/s) was also observed in each cycle in their experiment, but the variation of the flight speed was omitted from their discussion. Including the rotational body dynamics into the simulation model with a multiply linked body, Yokoyama *et al.* [24] discussed the effect of the abdominal motion and mass on the stability in butterflies flying forward, but the translation speed was constrained to be constant in the model. In a subsequent investigation of the free flight of a butterfly with a simulation model, this model was oversimplified in neglecting the clap-and-fling motion; the results might hence differ from those of the flight of a real butterfly [5]. Although researchers increasingly include the transient body dynamics into their analysis, the relation between the transient translation of a butterfly body and the unique flight behavior is not clearly explained. The discussion of the transient translation of the body motion is still not comprehensive, especially from the perspective of fluid dynamics.

The objective of our work was to investigate how the speed of a butterfly varies in forward flight and how that variation affects its motion and performance. To investigate the problem, with high-speed cameras we first recorded the forward flight of butterflies in the laboratory, then created a self-propulsion model of a butterfly to study the complicated interaction between the transient translation of the body and the surrounding air. In this self-propulsion model, the aerodynamic forces were recalculated in each iteration to define the velocity of body translation. The butterflies were released stationary and gradually increased their flight speed with the wing motion. The self-propulsion model was compared with the model in a constant inflow. We discuss the interaction between the unique flight motion of a butterfly and the variation of its speed of flight.

II. MATERIAL AND METHOD

A. Motion analysis of butterfly in forward flight

Fourteen leaf butterflies (*Kallima inachus*) were captured in the field and fed in the laboratory. The mean mass (W) of our samples was 0.40 ± 0.06 g; the wing span (S) was 6.50 ± 0.13 cm. We characterized and analyzed the motion and postures of the Indian leaf butterfly flying horizontally in a transparent experimental chamber. The forward flight might be defined as translation horizontally in space; because recording the precise forward flight of a butterfly in the laboratory experiment [15] is difficult, we redefined the forward flight such that the ratio between the vertical and horizontal translation is smaller than 0.2, $dz/dx < 0.2$, within a cycle. The wings and body motion of a butterfly were recorded with two synchronized high-speed cameras (Phantom v7.3 and Phantom v310), aligned orthogonally and operated

at 1000 frames per second with pixel resolution 1024×1024 . The wing and body kinematics of 40 individual flight cycles were recreated with our programs (developed in MATLAB). Further details of the method of motion analysis appear in our preceding articles [25–27].

B. Coordinate system of the flight kinematics

The motion of a butterfly in flight mainly couples the motions of wing flapping and rotation of the body. The body dynamics of a butterfly are vivid, and are observed to rotate periodically during free flight [17,21,28]. The abdominal motion of a butterfly yields a variation of the pitching angle of the thorax and is important for the stability of the flight [21,24]. By the rotation of the body, a butterfly manipulates the angle of the stroke plane and flapping downward and clapping backward during the down- and upstrokes, respectively. As the wing motion of a butterfly is much constrained because of the overlap between the fore and hind wings [6,28], it can scarcely perform a wing rotation in its flight. In this article we consider the wing motion to be a simple flapping motion. To describe the wing and body kinematics of a butterfly, we applied two coordinate systems: One is a global coordinate system (XYZ); its origin (O) is set at the initial center of mass (CM), not moving with the butterfly (Fig. 1). Axis X is defined therein as the direction in which a butterfly moves forward; axis Z is the direction opposite to that of gravity. The rotation of the body about axis Y is described with pitching angle $\beta(t)$, which is defined as the angle between the center line of the body and plane XY ; for instance, the pitching angle is zero when the body is lying in the plane, but is 90° when the body is vertical. The motion of the wings is connected with the butterfly body, and is simultaneous with the body in real flight. The body-fixed coordinate system ($X'Y'Z'$) is adopted to describe the wing-flapping motion (Fig. 1). The origin of the body-fixed coordinate system (O') is set at the wing base and translates and rotates with the body. The flapping motion is the rotation about axis X' ; the flapping angle is zero when the two wings clap together. In the forward flight of a butterfly, the

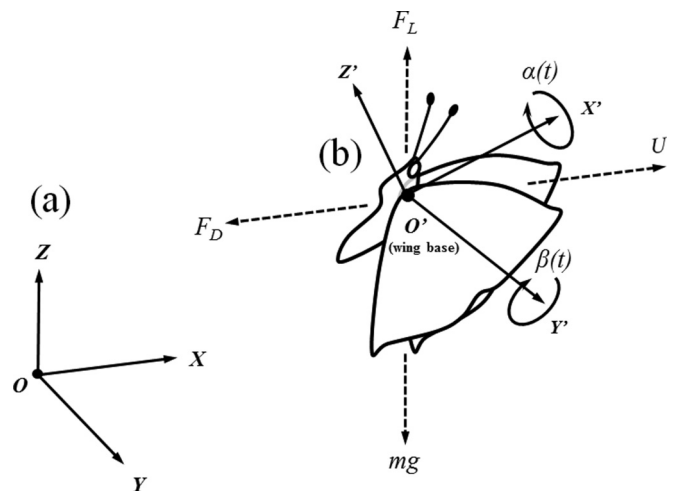


FIG. 1. Two coordinate systems to describe the motion of a butterfly: (a) global coordinates XYZ and (b) body-fixed coordinates $X'Y'Z'$.

translation of the insect is decomposable into two directions in the global coordinate system, axes X and Z . The velocities in directions X and Z are forward speed U and vertical speed V , respectively. Because of the symmetry of the geometry and the kinematics of a butterfly, the velocity in direction Y is reasonably neglected in the analysis. Analogously, the aerodynamic force generated opposite direction X is drag D ; the force generated in direction Z is lift L .

C. Wing and body kinematics of a butterfly

Figure 2 shows the wing and body kinematics of butterflies recorded in experiments on motion analysis. T is the flapping period and t/T is normalized time. The dashed line with error bars denotes flapping angle $\alpha(t)$; the solid line with error bars denotes the pitching angle of the body, $\beta(t)$. The data are averaged from 40 separate cycles; the error bars in the figure are means of the standard deviation (SEM). In the real flight of a butterfly, the flight motion is transient and uncontrollable, which leads to the wings and body kinematics being not exactly periodic functions. At the beginning of a stroke, the two wings clap together when the flapping angle is 0° ; the flapping angle begins to increase and attains maximum value 115° about $t/T = 0.55$; the wings then move back and clap again at the end of the stroke. The maximum wing speed occurs about $t/T = 0.25$ and 0.75 . The body of a butterfly is generally maintained at a large angle, and oscillates between 60° and 90° .

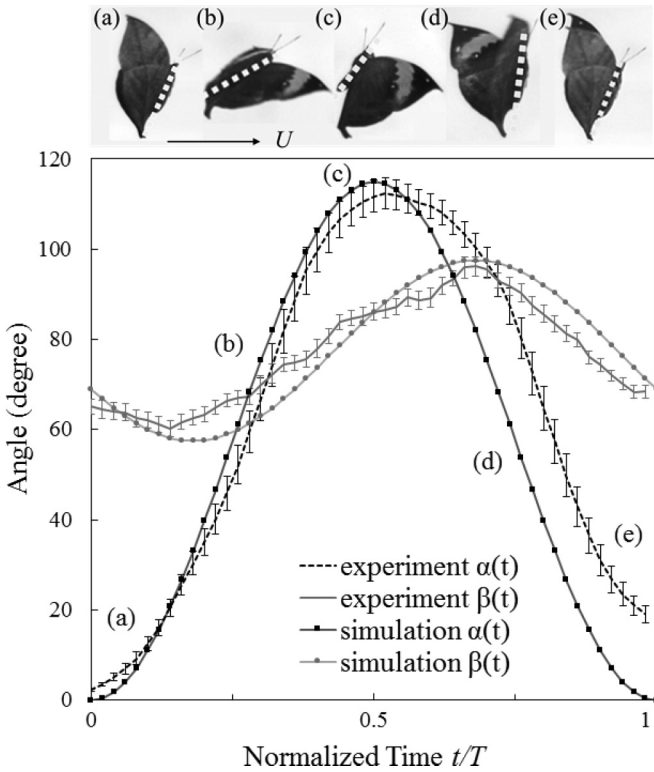


FIG. 2. Flapping and pitching angles; dashed lines with error bars and bold lines with error bars denote experimental data recorded in 40 individual cases (error bars = 1 SEM); bold lines with circles and squares are simplified functions of pitching angles and flapping angles for simulation. The photographs above the plot show the forward flight motion of a butterfly at varied time steps.

The angle of the body begins at 70° , and decreases gradually to a minimum, 60° , about $t/T = 0.20$. The body pitches up and the body angle increases gradually to 90° about $t/T = 0.70$.

To insert the flight kinematics of butterflies recorded from experiment into a simulation, two wave functions served to approach the flapping angle and pitching angle from experiment, expressed as

$$\alpha(t) = A_f - A_f \cos(2\pi f t), \quad (1)$$

$$\beta(t) = A_p \sin(2\pi f t) + B_0, \quad (2)$$

in which A_p and A_f are the amplitudes of flapping and pitching motions from the experiment. The flapping amplitude A_f of the wings is about 57.5° ; the amplitude of pitching angle A_p is about 20° . B_0 is the initial pitching angle of a butterfly body, which is 77.5° in our case. The mean flapping frequency f of an Indian leaf butterfly is about 10.79 ± 0.25 Hz; in the simulation, we used 10 Hz to represent the flapping frequency of this species. In Fig. 2, the simplified flapping and pitching angles used in the simulation are drawn as lines with circles and squares, respectively; the curves show a satisfactory correspondence between the simplified function and the experimental data. The rotating center of the body is set at the center of mass (CG).

The flapping angle specified above is relative to body-fixed coordinate system $X'Y'Z'$. A transformation between the global and body-fixed coordinate systems must be created to prescribe the flight kinematics in the simulation. The following transformation was adopted to create the flight kinematics of a butterfly based on the global coordinate system. The elementary rotation matrices of the body and wing motions are specified as

$$\mathbf{A}_{\text{body}} = \begin{bmatrix} c\beta(t) & 0 & s\beta(t) \\ 0 & 1 & 0 \\ -s\beta(t) & 0 & c\beta(t) \end{bmatrix}, \quad (3)$$

$$\mathbf{A}_{\text{flapping}} = \begin{bmatrix} 1 & 0 & 0 \\ 0 & c\alpha(t) & s\alpha(t) \\ 0 & -s\alpha(t) & c\alpha(t) \end{bmatrix},$$

in which matrix \mathbf{A}_{body} is the elemental rotation matrix of the body about axis Y ; matrix $\mathbf{A}_{\text{flapping}}$ is the elementary rotation matrix of the wing flapping about axis X' . $\alpha(t)$ and $\beta(t)$ are temporal functions of body pitching and wing flapping as mentioned above. The flight dynamics of a butterfly differ from those of other insects based on wing rotation; the rotation of the body leads to the variation of the stroke plane angle. Transformation matrix \mathbf{R} from a body-fixed coordinate system to a global coordinate system is expressed on multiplying the elemental matrices in this order:

$$\mathbf{R} = \mathbf{A}_{\text{body}} \cdot \mathbf{A}_{\text{flapping}}, \quad (4)$$

The angular velocity in the global coordinate system is calculated as the product of $d\mathbf{R}/dt$ and \mathbf{R}^{-1} :

$$\mathbf{s} = \frac{d\mathbf{R}}{dt} \cdot \mathbf{R}^{-1} = \begin{bmatrix} 0 & -\Omega_Z & \Omega_Y \\ \Omega_Z & 0 & -\Omega_X \\ -\Omega_Y & \Omega_X & 0 \end{bmatrix}, \quad (5)$$

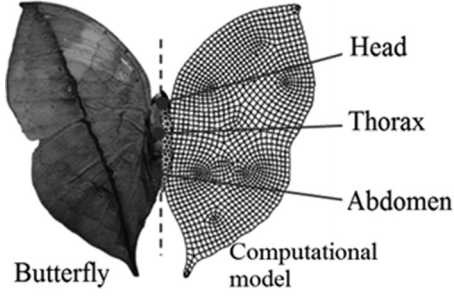


FIG. 3. Geometry of an India leaf butterfly and the computational model with mesh.

in which appear three components Ω_x , Ω_y , and Ω_z of angular velocity in the global coordinate system. The wing motion of a butterfly is presented as the three angular velocities in the global coordinate system.

D. Scheme of the simulation

Based on two-dimensional images of real butterflies, we created a butterfly model with software (PTC CREO 3.0). The relative motion of the abdomen and head was neglected; the head, thorax, and abdomen of the butterfly were simplified into one shuttle-shaped body. The wing span was 6.50 cm (Fig. 3). The butterfly was simplified as these three parts, and set as rigid bodies in the simulation.

The motion of the butterfly flying in air was simulated numerically with commercial software (ANSYS WORKBENCH). The equations governing the flow field include an equation for the three-dimensional, transient and incompressible continuity, and the Navier-Stokes equation,

$$\frac{\partial u_{f,j}}{\partial x_j} = 0, \quad (6)$$

$$\rho_f \left(\frac{\partial u_{f,j}}{\partial t} + u_{f,j} \frac{\partial u_{f,i}}{\partial x_j} \right) = - \frac{\partial p_j}{\partial x_j} + \mu \frac{\partial^2 u_{f,i}}{\partial x_j^2} + \rho_f f_{f,j}, \quad (7)$$

in which t denotes time, f_f body force, ρ_f fluid density, u_f velocity vector, p pressure, and μ dynamic viscosity. A semi-implicit method based on a finite-volume solver (FLUENT) was used to solve the flow; the pressure-linked equation (SIMPLE) algorithm with a second-order upwind scheme was applied to solve Eqs. (6) and (7). Each flapping cycle was divided into 250 time steps. The butterfly was bounded by air in a box ($15S \times 8S \times 8S$); the total mesh number was 5×10^7 with tetrahedral grids. The local remeshing skill was adopted for the moving surface of a butterfly during a simulation.

For the subsequent analysis we created models of two types—an anchor model and a self-propulsion model. The wing and body motions of the two models were prescribed with Eqs. (1) and (2). In the anchor model, the flight speed of a butterfly is constrained and treated as a constant inflow (U_{fixed}) from the boundaries, which is similar to a traditional CFD (computational fluid dynamics) computation [14,29]. In the self-propulsion model, the mass of the butterfly is set as 0.4 g in the simulation; the translation speed was set as zero at the beginning of the computation. The aerodynamic forces

were calculated on looping over the wing and body surfaces in the global coordinate system; the equation of motion was then applied to derive the translation speed, U . This speed is returned to the solver as a boundary condition of the wings and body in the next iteration. All outside boundaries are set as outlet. In the forward flight of a butterfly, the speed is insignificant in directions Y and Z ; the flight velocities in these two directions were hence ignored in the self-propulsion simulation.

III. RESULTS AND DISCUSSION

We make a comparison between data recorded from experiments in which motion was recorded and subjected to analysis and simulations with a self-propulsion model. The results of experiment and the self-propulsion simulation show a satisfactory correspondence in the flight speed and generation of the lift. The self-propulsion model is then compared further with the model fixed with a constant inflow.

A. Experimental observation of the forward flight of a butterfly

Figure 2 shows the flight motion of a butterfly in a cycle photographed with a high-speed camera. The flight speeds in vertical and horizontal directions were recorded with cameras for a butterfly in forward flight. Advance ratio J , which serves to characterize the normalized speed in the following article [30], is presented as

$$J = \frac{U}{2\alpha Sf}, \quad (8)$$

in which U denotes the flight speed in the horizontal or vertical direction; α is the flapping amplitude. $2\alpha Sf$ specifies the mean flapping velocity of the wing tip, which is 1.40 m/s in our case. The advance ratio is a dimensionless parameter commonly used to compare the flight speed to the flapping speed. In high-speed flight, the advance ratio is greater than 1; when the advance ratio is less than 0.1, the flight is treated as hovering [20]. The advance ratio was generally considered to be constant in stable forward flight [17,29,30], but, because of the variation of the flight speed, in the present work the advance ratio varied with time.

The upper and lower bold lines with error bars in Fig. 4 represent the advance ratio in horizontal and vertical directions, respectively; the horizontal dashed lines are the mean advance ratio \bar{J} averaged within a cycle. Figure 4 indicates that the advance ratio of the forward speed is oscillatory and has the form of a sinusoidal wave during the forward flight of a butterfly. Because of the variation of the flight speed, the advance ratio is not constant and oscillates with amplitude 0.4. At the beginning of a downstroke, for $t/T = 0-0.25$, the two wings are attached tightly and the body is maintained at a large angle; the flight speed has its maximum value, $J = 0.91$, about $t/T = 0.10$. The wings gradually open and the body pitches down; the speed gradually decreases and attains a minimum value, $J = 0.15$, at the end of the downstroke, $t/T = 0.55$. After the downstroke, the wings of a butterfly begin to close; the flight speed increases. The wings clap together again at the end of the upstroke and the advance ratio increases to 0.80 at the end of the cycle. The mean advance ratio of the species is

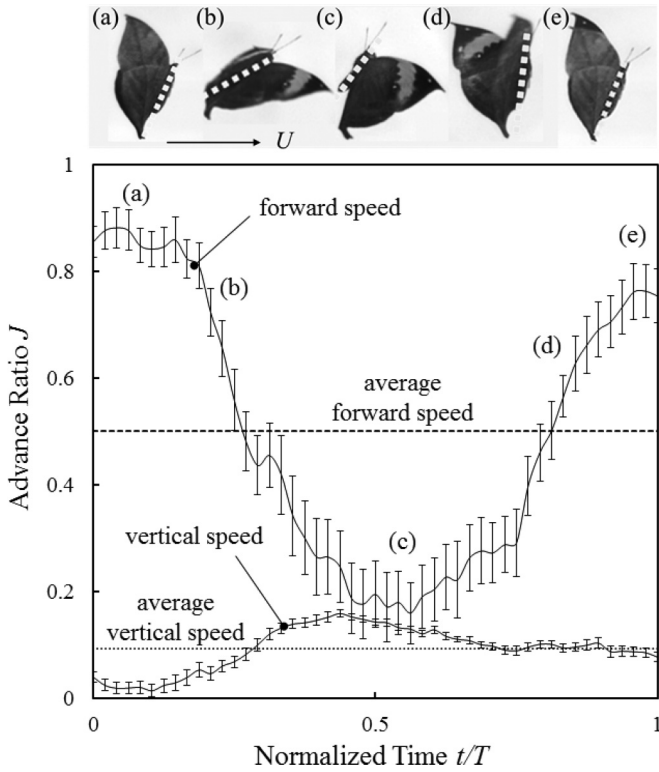


FIG. 4. Variation of advance ratio J and flight motion recorded from analysis of experimental motion. The solid lines with error bars represent the experimental data; the horizontal dashed lines represent the average advance ratio \bar{J} . Each error bar = 1 SEM; the flight velocity is normalized with the mean wing tip velocity (1.4 m/s).

0.50, $U = 0.70$ m/s, and the difference between the extrema is 0.75, $\Delta U = 1.05$ m/s. In contrast, the advance ratio of the vertical speed is small when a butterfly is in forward flight; the mean advance ratio is 0.09, $U = 0.14$ m/s. Through the modified definition of the forward flight (Sec. II A), only a slight vertical speed is recorded in our experiment. A butterfly transfers some energy from the horizontal to the vertical component, and produces an advance ratio at the end of a

stroke slightly smaller than that at its beginning. In real flight, the flight dynamic is transient and unstable, but, overall, the forward speed is five times the vertical speed; the variations of flight speed are almost periodic, which indicate that the flight motion in our experiment resembles stable forward flight.

B. Simulation of the forward flight of a butterfly

Our experimental data indicate that the forward speed largely oscillates when the butterfly undertakes forward flight; to understand further the influence of the transient flight speed on the flight performance, we generated a simulation model of a butterfly as self-propelling to investigate the aerodynamic performance. The flight speed and aerodynamic forces were recorded during the simulation.

Figure 5(a) shows the variation of the advance ratio for a butterfly self-propelled in air during the first six strokes. Consistent with an assumption of forward flight, the vertical displacement is much smaller than the horizontal displacement; the vertical translation is neglected in the model. In the self-propulsion model, the thrust generated is larger than the drag experienced in the early flight; the butterfly begins as stationary and gradually increases its flight speed (advance ratio) with the wing motion until the net drag is zero within a cycle. The mean advance ratio in each flapping cycle gradually approaches the mean advance ratio after becoming stable [Fig. 5(a)]. According to Fig. 5(a), the butterfly attains a condition of stable forward flight; the variation of advance ratio becomes periodic after the fifth stroke. In nature, for an animal stably moving forward or self-propelling, neither drag nor thrust is imposed on its body on average; the drag and thrust generated by a butterfly thus cancel within a cycle (drag-free) in a stable forward flight [17,31]. The net drag within a period approaches zero in the self-propulsion model after becoming stable. Figure 5(b) shows the variation of the advance ratio within a cycle after a butterfly flies forward stably; the tendency of the variation is similar to that recorded in the experiment (Fig. 5). The advance ratio has a maximum value 0.89, $U_{max} = 1.25$ m/s, at the beginning of the downstroke, and decreases quickly to a minimum, 0.17, $U_{min} = 0.24$ m/s, about the end of the downstroke, $t/T = 0.45$. The advance ratio increases

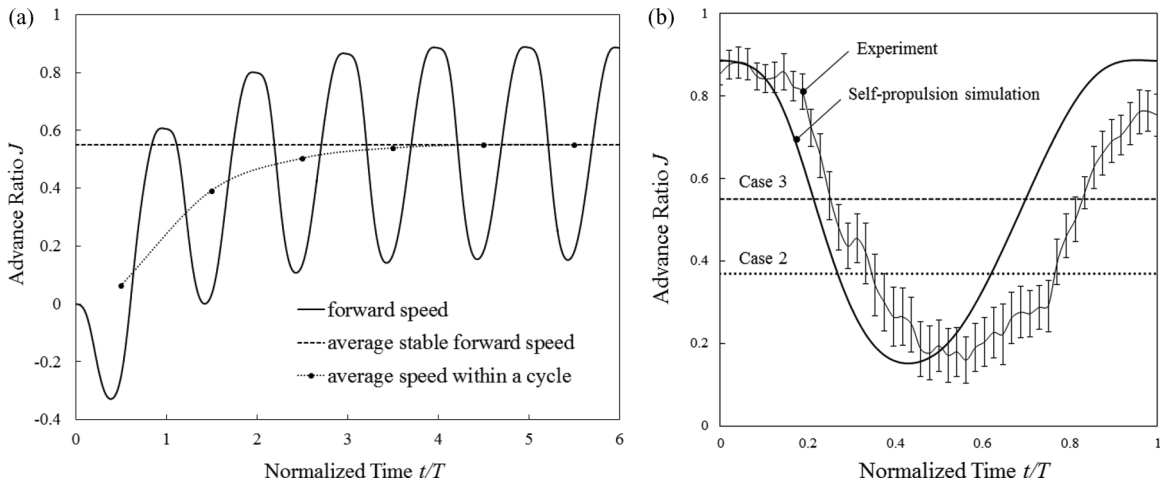


FIG. 5. Variation of advance ratio (normalized ratio) in self-propulsion simulation: (a) advance ratio in the first six periods; (b) variation of the flight speed within a cycle after becoming stable (see Supplemental Material [32]).

TABLE I. Summary of mean flight speed (\bar{U}), mean advance ratio (\bar{J}), net lift (\bar{L}), and net drag (\bar{D}) in simulation and experiment.

Model	\bar{U} (m/s)	\bar{J}	\bar{L}	\bar{D}
Case 1	0 (Constrained)	0	0.60	-0.82
Case 2	0.52 (Constrained)	0.37	1.05	-0.02
Case 3	0.77 (Constrained)	0.55	1.25	0.45
Case 4	0.97 (Constrained)	0.69	1.25	0.65
Self-propulsion	0.77	0.55	0.95	0.00
Experiment	0.70	0.50	1.00	0.00

again when the upstroke begins and attains a maximum, 0.89, at the end of the upstroke. The mean advance ratio in the self-propulsion model is 0.55, $\bar{U} = 0.77$ m/s, which is only one tenth larger than that recorded in the experiment. The net vertical force generated within a cycle is 3.73 mN, which is 94.5% of the the weight (3.924 mN). The results indicate the self-propulsion simulation is reliable and reflects accurately the flight of a butterfly.

To investigate the effect of the transient translation velocity of a butterfly in forward flight, we created anchored models with the same motion but varied the speed of inflow, and compared with the self-propulsion model. The flight speed of a butterfly is constrained and replaced with a varied constant inflow, $J = 0, 0.37, 0.55$, and 0.69 . Table I summarizes those data with the simulation and experimental data, including the mean advance ratio and average aerodynamic forces. The aerodynamic forces were normalized with the weight of the butterfly model. The conditions of cases and their physical meaning are explained as follows: In Case 1, the advance ratio is zero, which means that an aerodynamic force is generated only via the flapping motion and is independent of the flight speed. In Case 2, the advance ratio is 0.37; the drag-free condition is satisfied, which indicates that the butterfly flies stably forward at a constant speed. In Case 3, the advance ratio is set the same as the mean advance ratio of the self-propulsion mode; under this condition, the flyer is able to move as rapidly as when they are self-propelling. In Case 4, the advance ratio is greater than the mean advance ratio in the self-propulsion simulation; the aerodynamic forces are sensitive to the speed of flight of a butterfly, and both the drag and lift generated are proportional to the inflow speed: The greater is the inflow speed, the greater are the aerodynamic forces. Cases 2 and 3 are two ways typically applied to simplify the condition of forward flight when discussing an insect in such forward flight: First, the average flight speed is directly recorded in an experiment and then inserted into the simulation model as the inflow velocity (Case 3) [7,14,17]. Second, assuming that the insect is in stable forward flight, the generation of drag and thrust is zero within a cycle (Case 2).

Comparing Case 2 with the self-propulsion model, we find that both cases satisfy the condition drag free and can be treated as stable forward flight, but the advance ratio in Case 2 is 68% of the mean advance ratio in the self-propulsion model, which means that the butterfly in the condition of Case 2 is unable to fly as rapidly as according to the self-propulsion model. The net generated lift in both cases is near the weight of the butterfly model. In contrast, in Case 3, the advance ratio is set the same as the mean advance ratio of the self-propulsion model, but

the butterfly in this condition generates a large drag within a cycle; the normalized net drag is 0.45. In such flight conditions, the thrust generated by the motion of a butterfly is unable to overcome the body drag; the butterfly cannot maintain such a flight speed. In addition, the lift generated in Case 3 is five fourths the weight of a butterfly, which contradicts the basic assumption of forward flight, which is that the average lift equals the body weight. As a result, compared with the case of a constant flight speed, failing to consider the variation of flight speed might lead to an overestimate of the lift generated or an underestimate of the flight speed and thrust generated when a butterfly is in forward flight. The results in Table I indicate the importance of including the transient flight speed of a butterfly in forward flight.

Figure 6 compares the temporal history of lift and drag generated in Cases 2 and 3 and the self-propulsion model. A butterfly manipulates the angle of the stroke plane during flight: Its wings flap downward and generate both a drag and a lift in the downstroke; the wings clap backward and a thrust (negative drag) is contributed mainly in the upstroke. A slight negative lift is generated during the transition from downstroke to upstroke. The tendency of the variation of aerodynamic forces is similar to the reported results of a butterfly [5,14,24].

Because the flight speed varies in the self-propulsion case, it is locally greater or smaller than the flight speed in Cases 2 and 3, which produces large differences of the aerodynamic forces generated at various instants. Collectively, the advance ratio in the self-propulsion model is greater at the beginning and end of the downstroke, but smaller during the transition from downstroke to upstroke. Figures 6(a) and 6(b) compare the drag and lift between Case 2 and the self-propulsion model; the amplitudes of lift and drag variations are similar in the two cases. Even with a large advance ratio at the beginning of the downstroke [Fig. 5(b)], the aerodynamic forces are slightly larger in the self-propulsion model. Because of the decreased flight speed in the self-propulsion model, the aerodynamic forces decrease after $t/T = 0.25$. In Fig. 6(b), the drag generated decreases and converts to become a thrust about $t/T = 0.40$ in the self-propulsion case, which is earlier than that in Case 2. During $t/T = 0.60-0.85$, the flight speed increases in the self-propulsion model and is greater than that in Case 2; the thrust generated with self-propulsion is smaller than that in Case 2. The difference in lift generated is insignificant during the upstroke. The drag and lift generated in Case 3 and the self-propulsion model are compared in Figs. 6(c) and 6(d). The flight speed is larger in the self-propulsion model at the beginning of the downstroke, $t/T = 0-0.20$, but the force variations are almost the same in the two cases during this period. Because of the decreased flight speed, the lift and drag generated become smaller in the self-propulsion case after $t/T = 0.20$. The generation of a drag becomes a generation of thrust about $t/T = 0.40$; the thrust generated is significantly larger in self-propulsion during the transition from down- to upstroke, $t/T = 0.40-0.70$, and becomes inappreciable in the second half of the upstroke.

C. Interaction between flight speed and wing kinematics

The lift and drag generated are insensitive to the flight speed at the beginning of the stroke; among the three cases the

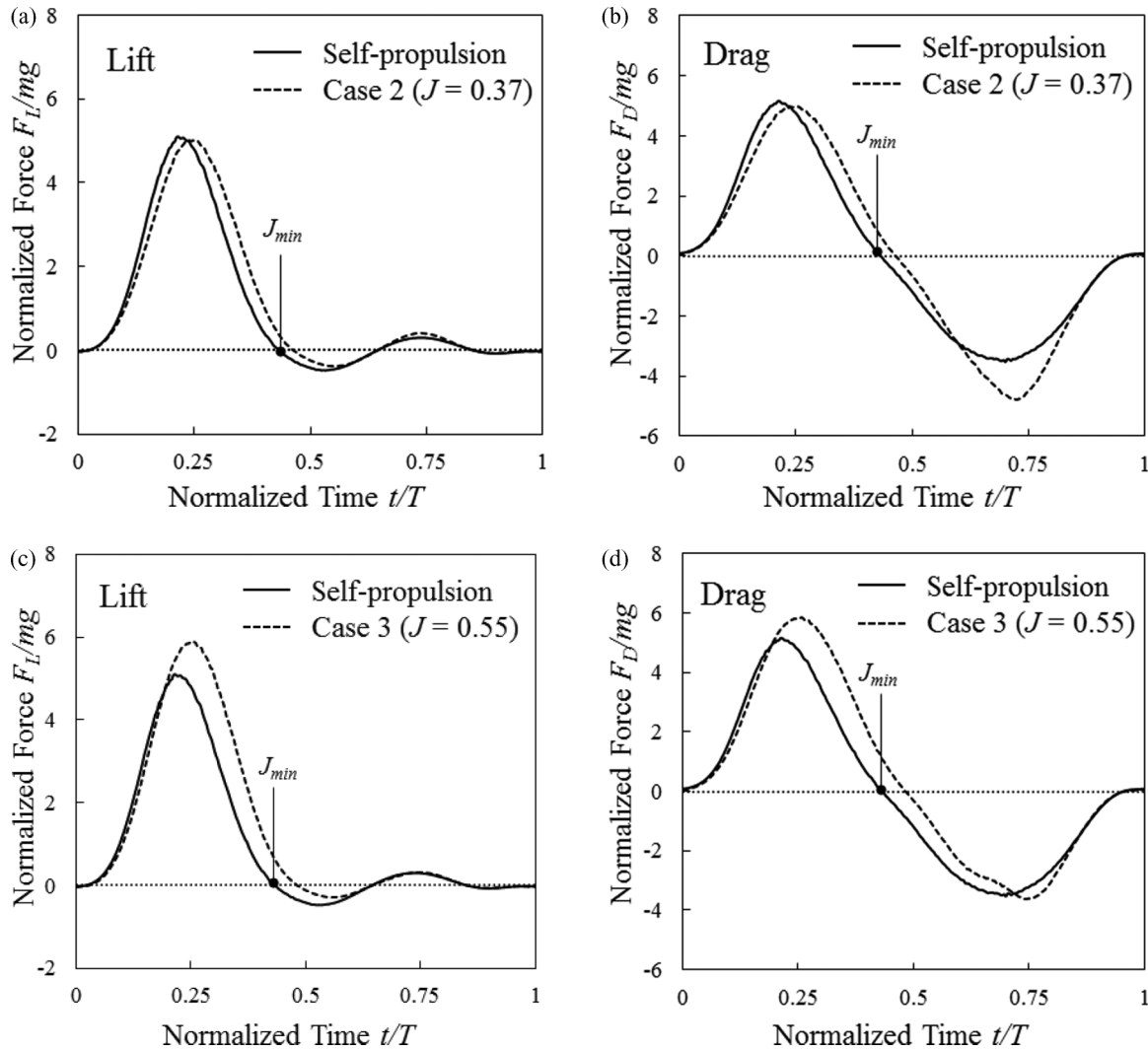


FIG. 6. Temporal history of normalized aerodynamic forces generated in various cases. J_{min} is the smallest advance ratio in the self-propulsion model.

variations of the lift and drag are almost the same during this period. The results indicate that the local large flight speed in the self-propulsion case does not significantly affect the aerodynamic forces generated. In contrast, the differences among the three cases become obvious when the flight speed decreases, $t/T = 0.25-0.75$; the self-propulsion model generates less drag but more thrust than in the other two cases after $t/T = 0.2$. The thrust generated occurs earlier and is significantly larger in the self-propulsion case at the beginning of the upstroke. In total, the self-propulsion model generates much less drag in the downstroke and is able to create a greater thrust during the transition region.

When the advance ratio increases, the relative velocity between the wing and the fluid generally also increases, and generates greater drag and lift, but the enhanced aerodynamic forces generated are imperceptible in the self-propulsion model at a large advance ratio. This unexpected result is connected to the unique wing kinematics of a butterfly. Preceding authors suggested that a clap-and-fling mechanism might result in enhanced lift, so that the fluid excluded from the clapping wing provides additional thrust for the insect [20,33].

The preceding work focuses on the interaction between the two wings; the clap-and-fling mechanism is hence called also a wing-wing interaction by several authors. A discussion excluding the flight speed might overlook another function of the clap-and-fling motion of an insect in forward flight. In forward flight a butterfly claps its wing tightly at the end of an upstroke and the beginning of a downstroke during which the flight speed is maximum during a cycle. When the wings clap together, the shape of the wings and body resembles a flat plate, which minimizes their projected area on the fluid [Fig. 7(a)]. With a small projected area, the form drag generated in this period is small, even when they translate at a large speed [Figs. 6(b) and 6(d)]. The clap motion of a butterfly enables that insect to move at a large speed in space without large drag generated accompanying an early downstroke, and enhances their average flight speed in the self-propulsion model. This investigation of a butterfly in forward flight produces an alternative interpretation of the clap-and-fling mechanism.

The flight speed is smaller in the self-propulsion case during the transition from downstroke to upstroke. The drag generated

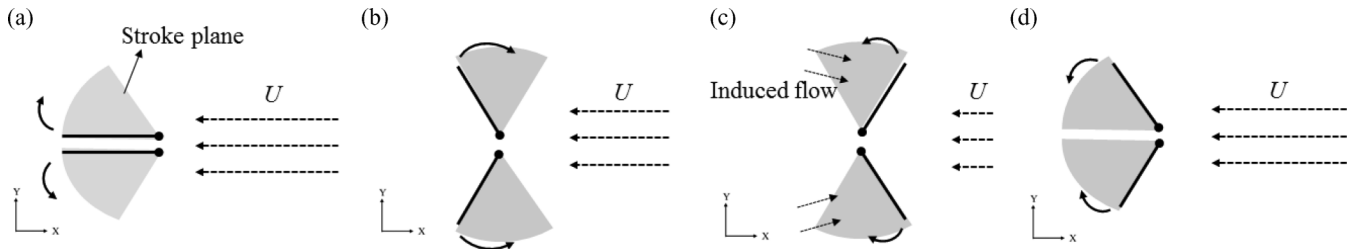


FIG. 7. Illustration of the clap-and-fling motion interacting with flight speed in the forward flight of a butterfly at (a) $t/T = 0-0.25$, (b) $t/T = 0.25-0.50$, (c) $t/T = 0.50-0.75$, and (d) $t/T = 0.75-1.00$; the lines terminating with spots represent the wings of a butterfly; the circle indicates the location of the wing base. Dashed arrows show the relative speed between a butterfly and a fluid, and bold arrows show the wing motion.

is smaller in the self-propulsion case at the middle of the downstroke; the thrust is generated earlier and is significantly larger at the beginning of the upstroke. The enhanced thrust generated is attributed to a *wake-capture* mechanism, which is proposed to explain the large lift generated during hovering of an insect or bird flight. In hovering flight, the reciprocating wing motion of the flapping wings causes a complicated interaction between the wings and the shedding vortex generated in the previous stroke. When the wing reverses its direction, it encounters a vortex generated in the preceding stroke and results in increased aerodynamic forces immediately after stroke reverse [9,10]. The complicated vortices generated around the wing would, however, rapidly shed into the wake region when the flyer is in forward flight. The insect captures neither vortices nor an induced flow from the wake during translation. The wake-capture effect is thus minor when the flight speed is large; for this reason the preceding discussion of the wake-capture effect is based mostly on a model of an insect hovering. In the self-propulsion model, the flight speed gradually decreases with the body drag during the middle of the downstroke [Fig. 6(b)]. Concurrently, the wing motion and speed of translation of a butterfly induce a strong flow behind the wing moving forward. The translation speed attains a minimum during the transition of a wing from downstroke to upstroke; the advance ratio has value 0.18, $U = 0.25$ m/s, at this time, which is near the condition of hovering. With a small

flight speed, the butterfly is thus able to capture the vortices shed from the downstroke.

Figure 8 shows the relative velocity in direction X between the fluid and the butterfly body. A strong forward flow is observed behind the wing in the self-propulsion case; when the wing starts moving back, the induced flow behind the wings impinges on the back surface of the wings and creates an additional thrust for a butterfly during the transition. Compared to Case 3, the butterfly translates forward at an increased speed during the transition; the relative speed between the induced flow and the butterfly is smaller than that in the self-propulsion case. This mechanism can explain that the thrust generated in the self-propulsion case is greater than that in Cases 2 and 3 during wing reversal. The wake capture was proposed to explain the aerodynamic forces generated in a hovering insect, but in the forward flight of a butterfly the minuscule flight speed during the wing reverse enables the insect to adopt the *wake-capture* mechanism, and further increases the thrust generated with the same motion.

The present results indicate the importance of considering the transient translation in the forward flight of a butterfly. The *clap-and-fling* motion enables a butterfly to fly at a large speed without significant drag being generated. The flight speed of a butterfly decreases much during the transition from downstroke to upstroke, and enables the butterfly to adopt the wake-capture mechanism during this period, so to

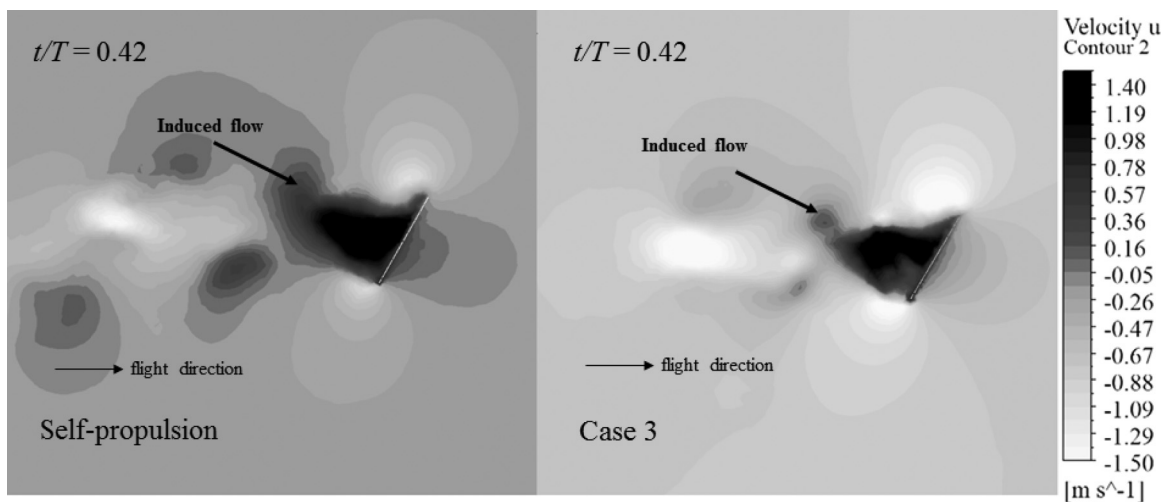


FIG. 8. Velocity of induced flow in direction X at $t/T = 0.42$, at which the advance ratio in the self-propulsion model is least within a cycle (the velocity in the figure is relative to the butterfly body).

enhance the thrust generated. The wing motion of a butterfly adroitly interacts with its transient flight speed, and improves the flight performance (flight speed and thrust generated) for a butterfly in forward flight. Compared with self-propulsion flight, considering flying at a constant speed might lead to either an underestimate of the flight speed and thrust generated or an overestimate of the lift generated, and might further lead to a misinterpretation of the performance of an insect's flight. The present investigation leaves scope for a future discussion. The size and mass of a butterfly can range over two orders of magnitude [34]. The flight performance and behavior of a butterfly likely vary with their size, mass, and even flapping frequency. The relation between the transient translation and the species of butterfly has not yet been answered. Also, a butterfly performs not only forward flight but also other transient flight motions such as takeoff or turning sharply; including the vertical transient translation in the discussion is hence necessary for the flight motion of this kind. These motions with a transient body translation and wing kinematics remain unclear and require future clarification.

IV. CONCLUSION

In this work, we investigated experimentally and computationally the transient translation of a butterfly in forward flight. A butterfly is observed to experience a large variation of flight speed within a cycle in the experiment, which contradicts an assumption of preceding authors who assumed a constant flight speed. Based on our experimental data, a self-propulsion simulation was created to verify the effect of the transient translation.

The results from the self-propulsion simulation are in satisfactory accordance with experimental data and are reliable. In the self-propulsion simulation, the mean flight speed is 0.75 m/s ($J = 0.55$) and with oscillation 0.55 m/s ($\Delta J = 0.39$). The shape of the variation of flight speed resembles a sinusoidal wave with a maximum, 1.25 m/s ($J = 0.89$), at the beginning of the downstroke, and a minimum, 0.24 m/s ($J = 0.17$), during the transition from downstroke to upstroke.

We compared also the self-propulsion model with a model with constant flight speed. Considering flying at a constant speed with the same motion, the maximum stable flight speed is 0.53 m/s ($J = 0.38$), which is only 68% that of the self-propulsion model. The butterfly moves more rapidly in air in self-propulsion than translating with a fixed flight speed. If we consider that the constant flight speed equals the mean flight speed of self-propulsion, although the butterfly is able to translate as rapidly as in the self-propulsion model, the thrust generated in the downstroke cannot overcome the body drag generated then. Also, the lift generated with a constant flight speed is greater than the weight of a butterfly, which prevents the butterfly from moving horizontally. In forward flight, the abrupt force generation causes a local maximum and minimum of the flight speed. When the flight speed is large, the butterfly attaches its wings tightly together to decrease the projected area and to reduce significantly the form drag. During the wing transition from downstroke to upstroke, the minuscule flight speed enables a butterfly to capture the induced flow generated in the downstroke. This *wake-capture* mechanism is observed in the forward flight of a butterfly; the thrust generated is hence significantly larger at the beginning of the upstroke.

For an insect with a small flapping frequency, considering flight at a constant speed leads to either an overestimate of the lift generated or an underestimate of the flight speed, and might further lead to misinterpretation of the flight performance of an insect's flight. The skillful interactions between the wing kinematics and the transient translation speed improve the flight performance of a butterfly in forward flight. The results indicate the importance of the transient translation for a flyer with a small flapping frequency, and might yield alternative insights into creating a MAV with small flapping frequency in the impending future.

ACKNOWLEDGMENT

The Ministry of Science and Technology, R.O.C. partially supported this work under Contract No. MOST 103-2221-E-002-059-MY03.

-
- [1] C. P. Ellington, C. van den Berg, A. P. Willmott, and A. L. R. Thomas, *Nature* **384**, 626 (1996).
 - [2] M. H. Dickinson, F. O. Lehmann, and S. P. Sane, *Science* **284**, 1954 (1999).
 - [3] J. M. Birch and M. H. Dickinson, *J. Exp. Biol.* **206**, 2257 (2003).
 - [4] H. Liu, C. P. Ellington, K. Kawachi, C. van den Berg, and A. P. Willmott, *J. Exp. Biol.* **201**, 461 (1998).
 - [5] K. Suzuki, K. Minami, and T. Inamura, *J. Fluid Mech.* **767**, 659 (2015).
 - [6] H. Tanaka and I. Shimoyama, *Bioinspiration Biomimetics* **5**, 026003 (2010).
 - [7] K. Senda, T. Obara, M. Kitamura, N. Yokoyama, N. Hirai, and M. Lima, *Bioinspiration Biomimetics* **7**, 025002 (2012).
 - [8] W. Shyy and H. Liu, *AIAA J.* **45**, 2817 (2007).
 - [9] K. B. Lua, T. T. Lim, and K. S. Yeo, *Exp. Fluids* **51**, 177 (2011).
 - [10] S. P. Sane and M. H. Dickinson, *J. Exp. Biol.* **205**, 1087 (2002).
 - [11] M. H. Dickinson, F. O. Lehmann, and K. G. Gotz, *J. Exp. Biol.* **182**, 173 (1993).
 - [12] F. O. Lehmann, S. P. Sane, and M. Dickinson, *J. Exp. Biol.* **208**, 3075 (2003).
 - [13] T. Maxworthy, *J. Fluid Mech.* **93**, 47 (1979).
 - [14] L. Zheng, T. L. Hedrick, and R. Mittal, *PLoS One* **8**, e53060 (2013).
 - [15] A. K. Brodsky, *J. Exp. Biol.* **161**, 77 (1991).
 - [16] M. Fuchiwaki, T. Kuroki, K. Tanaka, and T. Tababa, *Exp. Fluids* **54**, 1450 (2013).
 - [17] H. Nagai, K. Isogai, T. Fujimoto, and T. Hayase, *AIAA J.* **47**, 730 (2009).
 - [18] W. Shyy, H. Aono, C. K. Kang, and H. Liu, *An Introduction to Flapping Wing Aerodynamics* (Cambridge University Press, New York, 2013).
 - [19] R. Dudley and R. B. Srygley, *J. Exp. Biol.* **191**, 125 (1994).
 - [20] C. P. Ellington, *J. Exp. Biol.* **202**, 3439 (1999).
 - [21] S. Sunada, K. Kawachi, I. Watanabe, and A. Azuma, *J. Exp. Biol.* **183**, 249 (1993).
 - [22] R. B. Srygley and A. L. R. Thomas, *Nature* **420**, 660 (2002).

- [23] H. Takahashi, H. Tanaka, K. Matsumoto, and I. Shimoyama, *Bioinspiration Biomimetics* **7**, 036020 (2012).
- [24] N. Yokoyama, K. Senda, M. Iima, and N. Hirai, *Phys. Fluids* **25**, 021902 (2013).
- [25] Y. H. Chang, S. C. Ting, J. Y. Su, C. Y. Soong, and J. T. Yang, *Phys. Rev. E* **87**, 022707 (2013).
- [26] J. Y. Su, S. C. Ting, Y. H. Chang, and J. T. Yang, *Phys. Rev. E* **84**, 012901 (2011).
- [27] Y. H. Chang, S. C. Ting, C. C. Liu, J. T. Yang, and C. Y. Soong, *Exp. Fluids* **51**, 1231 (2011).
- [28] R. Dudley, *The Biomechanics of Insect Flight: Form, Function, Evolution* (Princeton University Press, Princeton, NJ, 2000).
- [29] M. Sun and J. H. Wu, *J. Exp. Biol.* **206**, 3065 (2003).
- [30] C. P. Ellington, *Philos. Trans. R. Soc., B* **305**, 41 (1984).
- [31] E. Christophe, *J. Fluid Struct.* **30**, 205 (2012).
- [32] See Supplemental Material at <http://link.aps.org/supplemental/10.1103/PhysRevE.92.033004> for a butterfly in forward flight in real flight and simulation.
- [33] C. P. Ellington, *Philos. Trans. R. Soc., B* **305**, 79 (1984).
- [34] R. Dudley, *J. Exp. Biol.* **150**, 37 (1990).